# *Digital Temperature Control Project Using Peltier Modules to Improve the Maintenance of Battery Lifetime*

A. K. R. Sombra, F. C. Sampaio, R. P. T. Bascopé, B. C. Torrico
Electrical Engineering Department
Federal University of Ceará
Fortaleza, Ceará
E-mail: andresakelly@hotmail.com, felipecsamp@hotmail.com, rene@dee.ufc.br, bismark@dee.ufc.br

***Abstract*— The lifetime of a battery depends mainly on the operating temperature. Thus, this paper proposes a low cost refrigeration system applied to batteries temperature control. In the proposed system, Peltier modules (thermoelectrical devices, which uses the Peltier effect for heat exchange) are used to refrigerate the system. In addition are compared the performance of two control strategies (conventional PI and P+I), applied to the system temperature control. It is shown that the P+I controller has a better performance than the conventional PI controller due to its characteristic of present higher control effort at the initial time. It is proposed, though, a structure with the P+I controller to correct the windup problem. Moreover, the transfer function of the system was obtained applying a system identification method, in order to improve the control precision and to reduce the complexity in obtaining the system model. The prototype is still in development stage, in this way, the results were obtained by simulation.**

***Keywords*— Thermoelectric, Peltier, battery, lifetime, temperature, control, anti-windup.**

## I. INTRODUCTION

In the last years, with the increasing number of photovoltaic system applications, like telecommunication towers, water pumping, remote lighting, the demand for batteries had a significantly increase[1]-[5]. Thus, it is important to pay attention to the lifetime batteries.

However, the batteries operating temperature is a critical factor for its lifetime. The operating temperature affects the chemical activity and the internal resistance of the battery. At higher temperatures, the internal resistance decreases, consequently, the discharge voltage increases. In this context, the Ampère-hour capacity of the battery also increases. In the other hand, elevated temperatures increase the chemical activity, accelerating the discharge time of the battery. Each type of battery presents a different operating temperature. However, in general, the best performance of a battery is achieved at an operating temperature between 20 °C to 40 °C [6]-[7].

In VRLA (Valve Regulated Lead Acid) batteries, for example, operation at high temperature causes loss of water and accelerates the dry-out, which leads to loss of capacity. Thus, the lifetime of a VRLA battery dramatically decreases in 40 °C of operating temperature, for example. For this reason, the operating temperature of a VRLA battery is between 20 °C and 25 ° C. [8]-[9]

In this context, the objective of this paper is to present a low cost system for batteries temperature control utilizing thermoelectrical modules, aiming the maintenance of its lifetime.

Peltier module is a thermoelectrical energy converter, which consists of a bunch of semiconductors connected in series and positioned in such a way to produce heat transfer from one side to another of the module. To realize the conversion of electrical energy to thermal energy, Peltier modules utilize the Peltier effect (characteristic effect of semiconductors). This effect allows that the injection of a current by the module terminals induce the heat transfer from the hot side to the cold side of the module [10]-[12].

Peltier Modules were chosen as heat transfer, due to its advantages, like: simple manipulation, reduced size and reduced weight, in relation to other refrigeration systems, that, many times, use fluids (like air and water) to refrigerate. Moreover, Peltier modules are powered by DC sources [8].

Other works have been utilized Peltier modules for temperature control in different applications [13]-[15]. This paper uses a system identification method to obtain the system transfer function, with the objective of decrease the complexity in obtaining the model of the process and improve the control precision. This paper also compares the performance of two control strategies: conventional PI and P+I for this application.

The proposed prototype is in development stage. For this reason, all the results presented, in this version of this paper, were obtained by simulation.

## II. System Identification

### A. Introduction to System Identification

In order to control a process, it must know the relationship between the input and output of the plant, which is defined as the mathematical model of a system representing its essential aspects as appropriate for a particular use [16].

It is possible then to find it in two different ways: the physical-mathematical analysis, which are interpretative equations of physical phenomena that characterize the process in question or the system identification, which involves the application of an entry in the real plant yielding a corresponding output to the applied input. It can find a representative system model from the obtained output by several possible methods.

In this work, the mathematical model of the system becomes very complex because of the need to accurately model the dynamics of the whole plant, not just one Peltier module. Thus, it was decided to obtain the system transfer function, using a system identification method, in view of the experimental model represents sufficiently well the dynamics of the system, in addition to being a simpler option for obtaining the function transfer system to be controlled.

According to [17], obtaining a plant transfer function using identification system consists of four steps: Input/output data acquisition under an experimentation protocol, Selection or estimation of the "model" structure (complexity), Estimation of the model parameters, validation of the identified model.

### B. Real Plant and Identification Procedure

The plant consists of a 60 L of polystyrene with cover, with two thermoelectric modules allocated at the top rear of the Styrofoam. The aforementioned modules consist of Peltier thermoelectric associated with a heat sink and a cooler on each side of the thermoelectric. It notes that the external and internal heat sinks have heat insulation between them, so that the temperature does not influence one another by radiant heat.

The model used was the 50 W thermoelectric TEC1 - 12706 [18], depicted in Figure 1. To the measurement of plant internal temperature it was used the integrated circuit LM35 [19].

The developed plant is shown in Figure 2.

As mentioned, the aim is to control, from the initial temperature, the temperature variation between the outside and the inside, in order to impose the desired internal temperature. However, to achieve the desired temperature variation, one needs to know the current which must be applied to the plant.

Thus, to perform the experimental analysis of the plant model, it was applied a current step and the internal temperature was measured. The applied step was 2.95 A, which corresponds to approximately half the nominal load of the modules.


Figure 1. TEC – 12706.

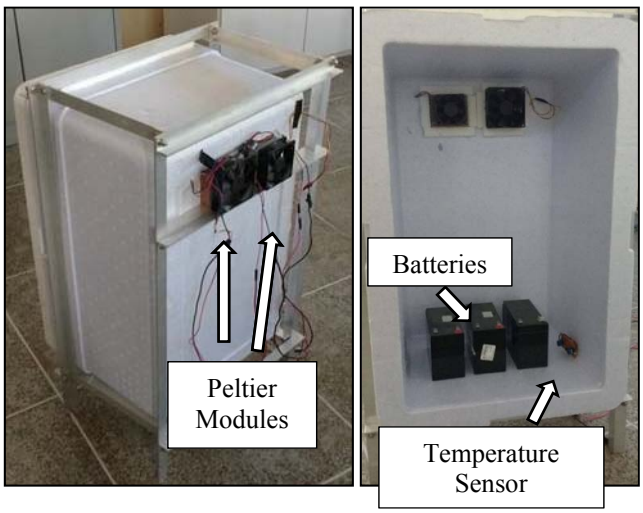


Figure 2. Developed Plant.

To choose the sampling time Ts, it was used the criterion set out in Equation 1 [17]:

$$\frac{T_0}{4} < T_s < T_0 \qquad (1)$$

where $T_0$ corresponds to the time constant in closed loop. The sampling time was set at 15 sec.

At an initial temperature of 23 ° C, it was acquired the step response, applied after the first sampling period.

From the response of to the real plant rung shown in Figure 3, it can bring the plant to a first order model in Equation 2 format.

$$G(s) = \frac{K}{a_1 s+1} \qquad (2)$$

where $a_1$ corresponds to the time constant in closed loop.

It can represent the plant model as a first order model in the form of Equation 1:

$$Y(s) = G(s)U(s) \qquad (3)$$

where Y(s) is the system output and U(s) the input step. Therefore:

$$U(s) = \frac{A}{s} \qquad (4)$$

where K is the gain of the plant and $a_1$ is the time constant of the model.

A linear time-invariant system (LTI) with an input and an output (SISO - Single Input Single Output) can be described as in Equation 2 [21].

$$y(\infty) = \lim_{s \to 0} sY(s) = K.A \qquad (5)$$

Note that y (∞) is the temperature variation in the steady state, so it must adjust the gain K according to Equation 5.

$$K = \frac{y(\infty)}{A} = \frac{Temperature_{final} - Temperature_{initial}}{A} \qquad (6)$$

From Eq 6, it was calculated the gain K of the plant: -3.57.

To obtain the time constant a1, it uses the Equation 7 [17], where a1 is the time corresponding to the value found Va in Eq. 7.

$$V_a = 0.63[y(\infty) - y(0^-)] + y(0^-) \qquad (7)$$

From Eq. 7 relates to Eq. 8.

$$Va = 0.63[Temp_{final} - Temp_{initial}] + Temp_{initial} \qquad (8)$$

With Eq.8 it is calculated the time constant, a1: 600

The final model of the plant is shown in Equation 9.

$$G(s) = \frac{-3.57}{600s+1} \qquad (9)$$

To validate the model, Figure 3 compares the step response of the model with the step response of the real plant.

It was calculated the model error encountered sample to sample, obtaining then the average error. The average error obtained was 0.89%, which is considerably acceptable. It was found that in any sample was recorded error greater than 4% and only 5 of 352 samples had higher errors than 3%.

## III. CONTROLLER DESIGN

### A. *Discretization of the Model and Theoretical Foundation*

The model is initially discretized by ZOH method (zero-order hold), presented by Equation 10 [16]:

$$G(z) = (1 - z^{-1})Z\left\{\frac{G(s)}{s}\right\} \qquad (10)$$

The discretized plant is shown in Eq. 11:

$$G(z^{-1}) = \frac{-0.08809z^{-1}}{1-0.9753z^{-1}} \qquad (11)$$

It is possible to control the first order plant with a conventional PI controller. However, being a thermal system, and thus a very slow system, it is desired that the initial control effort be as high as possible, which does not occur with the conventional PI, as will be explained in Topic C.

The block diagram of PI controller is shown in Figure 4. For purposes of differentiation, the controller of Figure 4 can be called a P + I controller.

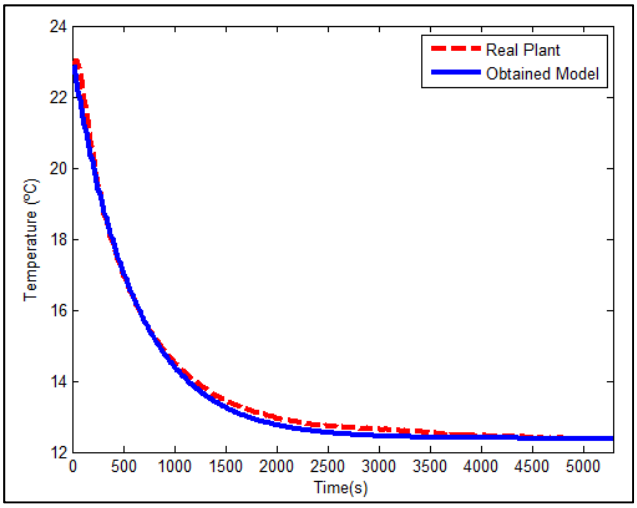


Figure 3. Comparison between Obtained Model and Real Plant.

It is observed that the Integrator block inserts a zero at the origin. To rule out the effect of zero defines the desired pole of the inner loop located at the origin. It is called the innermost loop as $G_i(z^{-1})$.

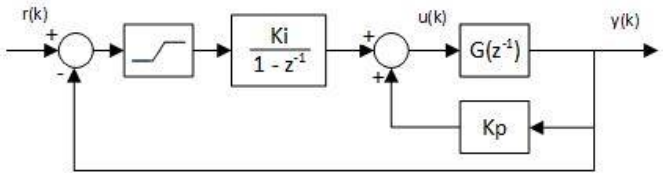


Figure 4. Block diagram of P+I Controller

Figure 5 shows the block diagram of Figure 5 simplified, where $G_i(z^{-1})$ is defined in Equation 12.

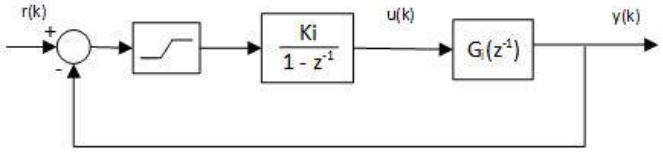


Figure 5. Simplified block diagram with the P + I controller.

$$G_i(z^{-1}) = \frac{G(z^{-1})}{1-K_p.G(z^{-1})} \qquad (12)$$

Therefore, it is possible to obtain the gain Kp according to the characteristic equation of the loop $G_i(z^{-1})$, according to Equation 13, setting the desired pole, which was selected as located at the origin.

$$1 - K_p.G(z^{-1}) = 0 \qquad (13)$$

Thus, find the gain Kp according to Equation 14.

$$K_p = \frac{1}{G(0)} = \frac{0-0.9753}{-0.08809} = 11.0716 \qquad (14)$$

The outer loop pole is set according to the desired requirements for closed-loop system, as response time for 95% (5% error) for 5 minutes. The 95% response time is defined according to Equation 15 [20]:

$$t_{5\%} = 3\tau \quad (15)$$

where $\tau$ is defined as the closed-loop time constant.

From a desired continuous plant, it is possible to find the desired pole according to the operator $z$ relation to the time constant $\tau$. When equal to zero the denominator of Equation 2 is the desired pole SD by Equation 16.

$$s_d = -\frac{1}{\tau} \quad (16)$$

It is known that the $z$ operator may be defined according to Equation 17 [17].

$$z = e^{s.T_s} \quad (17)$$

Thus, the desired discrete pole can be related by Equation 18.

$$p_d = e^{s_d.T_s} \quad (18)$$

where $p_d$ correspond to the desired pole of the outer loop.

It is estimated, then the desired pole from equations 15 and 16, $p_d = 0.8607$.

It is defined as $H_i(z^{-1})$ the block integrator of Figure 5.

The closed loop system transfer function can be defined by the equation 19.

$$H(z^{-1}) = \frac{H_i(z^{-1}).G_i(z^{-1})}{1+H_i(z^{-1}).G_i(z^{-1})} \quad (19)$$

Thus, $K_i$ is defined according to the system characteristic equation, Equation 20, and performed according to the definition of the desired pole.

$$1 + \frac{K_i}{(1-z^{-1})}.G_i(z^{-1}) = 0 \quad (20)$$

The gain $K_i$ is defined in Eq. 21.

$$K_i = \frac{-1(1-1/p_d)}{G_i(p_d)} = -1.5812 \quad (21)$$

## B. Proposed Anti-windup Structure

For the control, it is proposed to P+I controller refurbished in stable functions in order to imply the integrator to correct possible wind-up problems. Thus, the controller shown in Figure 4 is redesigned according to Figure 6.

This anti-windup correction is only performed correctly depending on the allocation to the saturator block.

In section IV, the two controllers will be compared, the P+I, corresponding to Figure 4 and the anti-windup P+I, corresponding to Figure 6.

However, the controller design is the same for both controllers.

It is then possible to obtain the closed loop transfer function of block diagram of Figure 6, shown in Equation 22.

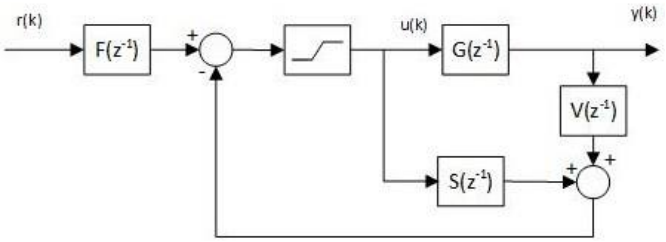


Figure 6. Block Diagram of the Anti-windup P+I.

$$H(z^{-1}) = \frac{F(z^{-1}).B(z^{-1})}{A(z^{-1})+A(z^{-1}).S(z^{-1})+V(z^{-1}).B(z^{-1})} \quad (22)$$

where $A(z^{-1})$ and $B(z^{-1})$ corresponding to the denominator and the numerator of the discretized plant, respectively, defined by Equations 23 and 24.

$$A(z^{-1}) = 1 + a_1.z^{-1} \quad (23)$$

$$B(z^{-1}) = b_1.z^{-1} \quad (24)$$

where $a_1$ and $b_1$ are known, according to discrete plant.

Through comparison between the block diagrams of Figures 4 and 6, are defined in terms of $K_p$ e $K_i$, the polynomials $S(z^{-1})$,$V(z^{-1})$ and $F(z^{-1})$ in the Equations 25, 26 e 27.

$$S(z^{-1}) = -z^{-1} \quad (25)$$

$$V(z^{-1}) = (K_i - K_p) + K_p.z^{-1} \quad (26)$$

$$F(z^{-1}) = K_i \quad (27)$$

The obtained closed-loop transfer function is shown in Eq. 28.

$$H(z^{-1}) = \frac{0.1393z^{-2}}{1-0.8607z^{-1}} \quad (28)$$

## C. Adjust the Conventional PI Controller for Comparison with the P+I Controller

The block diagram of the conventional PI controller is shown in Figure 7.

The controller in Figure 7 may be remodeled according to the RST model [17], as shown in Figure 8.

The closed loop transfer function of the block diagram of Figure 8 is shown in Equation 29.

$$H(z^{-1}) = \frac{T(z^{-1}).B(z^{-1})}{A(z^{-1}).S(z^{-1})+R(z^{-1}).B(z^{-1})} \quad (29)$$

For a comparison between controllers to be actually valid, there must be the same system requirements of the closed loop. The desired plant is found from a discretized continuous plant, obtained from the selected requirements [17]. The discrete desired plant is shown in Equation 30.

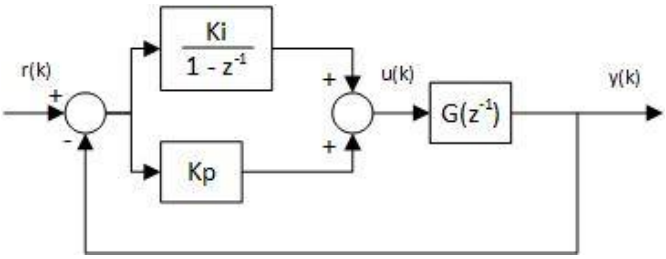


Figure 7. Conventional PI Controller Block Diagram.

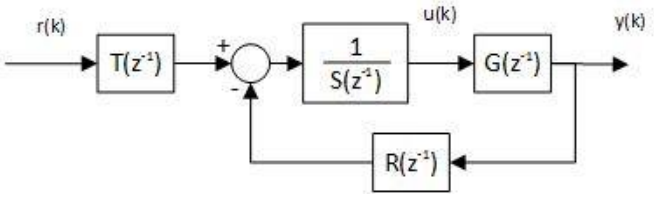


Figure 8. Conventional PI Controller in the RST Format.

For a comparison between controllers to be actually valid, there must be the same system requirements of the closed loop. The desired plant is found from a discretized continuous plant, obtained from the selected requirements [17]. The discrete desired plant is shown in Equation 30.

$$\mathrm{Hd}(z^{-1}) = \frac{-0.01491 - 0.01349z^{-1}}{1 - 1.712z^{-1} + 0.7408z^{-2}} \quad (30)$$

It defines the polynomial P ($z^{-1}$) as the denominator of the desired plant [17] shown in Equation 31.

$$\mathrm{P}(z^{-1}) = 1 + p_1.z^{-1} + p_2.z^{-2} \quad (31)$$

Where $p_1$ and $p_2$ are known, according to discrete desired plant defined in Equation 30.

By comparing the diagram of Figure 7 and Figure 8, it obtain the orders of polynomials, defined by equations 32 and 33.

$$\mathrm{S}(z^{-1}) = 1 - z^{-1} \quad (32)$$

$$\mathrm{R}(z^{-1}) = r_0 + r_1.z^{-1} \quad (33)$$

The polynomial $\mathrm{T}(z^{-1})$ is set so as to maintain the static gain of the closed loop unit according to the Equation 35.

According to Equation 34, the static gain of a discrete function is defined as z = 1.

$$\mathrm{z} = e^{s.Ts} = e^{0.Ts} = 1 \quad (34)$$

Thus, the static gain of the closed loop function of Equation 29 is given by Equation 35:

$$\mathrm{H}(1) = \frac{\mathrm{T}(1)}{\mathrm{R}(1)} \quad (35)$$

Thus, for H(1) is equal to 1, defines the polynomial $\mathrm{T}(z^{-1})$ as a gain calculated from the sum of the polynomial coefficients $\mathrm{R}(z^{-1})$, as shown in Equation 36.

$$\mathrm{T}(z^{-1}) = r_0 + r_1 \quad (36)$$

Comparing the denominator of Equation 29, also called Bezout Equation [17] with the polynomial P ($z^{-1}$) are obtained the Equations 37 and 38.

$$r_1 = \frac{p_2 + a_1}{b_1} \quad (37)$$

$$r_0 = \frac{p_1 - a_1 + 1}{b_1} \quad (38)$$

The polynomials are obtained according to the equations that relate, shown in Equations 39 and 40. The polynomial $\mathrm{P}(z^{-1})$ was set in Equation 30.

$$\mathrm{R}(z^{-1}) = -2.9843 + 2.6618z^{-1} \quad (39)$$

$$\mathrm{T}(z^{-1}) = -0.3225 \quad (40)$$

The obtained closed loop function is shown in Eq. 41.

$$\mathrm{H}(z^{-1}) = \frac{0.02841}{1 - 1.712z^{-1} + 0.7408z^{-2}} \quad (41)$$

The main difference between the P+I controller and the conventional PI controller is given in the control signal, as the P+I controller reaches the maximum at the start of the reference signal. The Section IV will expose such difference.

## IV. Simulation Results

To simulate the system response closed loop, reference is applied as the desired temperature variation. It is assumed, though, an initial temperature of 25 ° C, which is coupled both to the output as the reference, in order to better visualize the plant output.

Since the model of the thermoelectric used supports a maximum current of 6.4 A, in the simulation, is added a saturation of 6.4 in the controller output.

Figures 9 to 11 were obtained for a desired temperature variation of -10 ° C, which results in the required temperature 5 ° C.

The system output, the control signals of PI and P+I controllers and the applied reference are shown in Figure 9. For comparison between PI and P+I controller, the saturation is neglected in Figure 9 and in Figure 10.

It can be seen, in Figure 9, the difference between the control signals PI and P + I. The control signal controller P + I begins at maximum. This feature is crucial for the rejection of disturbance. It can be also observed a small difference between the system outputs using P+I controller and using the PI controller. This difference is due to the adjustment of the controllers, which was carried out so that the responses of the systems were the closest possible to the two controllers, but the outputs are not strictly equal.

A disturbance is applied to the output of the plant to verify the difference between the rejection of disturbance of the PI controller and the P + I controller.

Figure 10 shows the disturbance applied at the time 1500 s, the outputs of the systems and control signals of the P+I and PI controllers.

Considering a margin of ± 5% of the reference value, it can be observed, in Figure 10, that after the disturbance, the system output using P+I controller stabilizes about 4 minutes faster than the system using the PI controller.

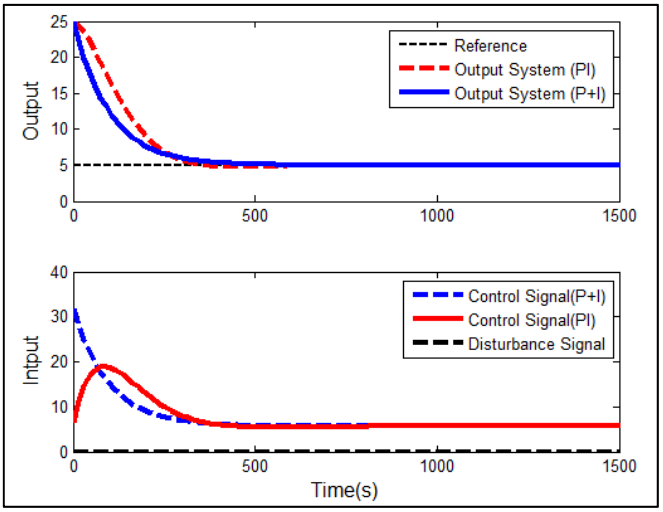


Figure 9. System Output, Control Signals (PI e P+I) and the Applied Reference.

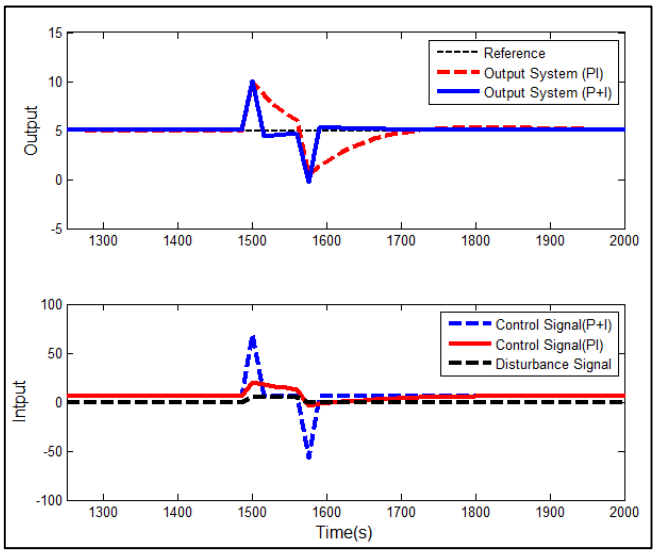


Figure 10. System Outputs (PI and P+I), Control Signals (PI and P+I) and the Disturbance Signal.

Therefore, the most appropriate controller for the application in question is the P+I controller.

Then, consider the plant input saturation and compared P+I controller, shown in Figure 4, and the P+I controller anti-windup, shown in Figure 6.

Figure 11 shows the system output, the control signal to the P+I controller and the anti-windup P+I controller. The disturbance applied and the reference is also shown in Figure 11. The disturbance was applied at time 1500 sec.

From Figure 11, it can be seen that the proposed anti-windup P+I controller has better performance because stabilizes approximately 44 minutes faster than the P+I controller of Figure 4. It is also noted that the system controller using P+I of Figure 4 shows strong non-linear characteristic, with windup both reference tracking as the rejection of disturbance.

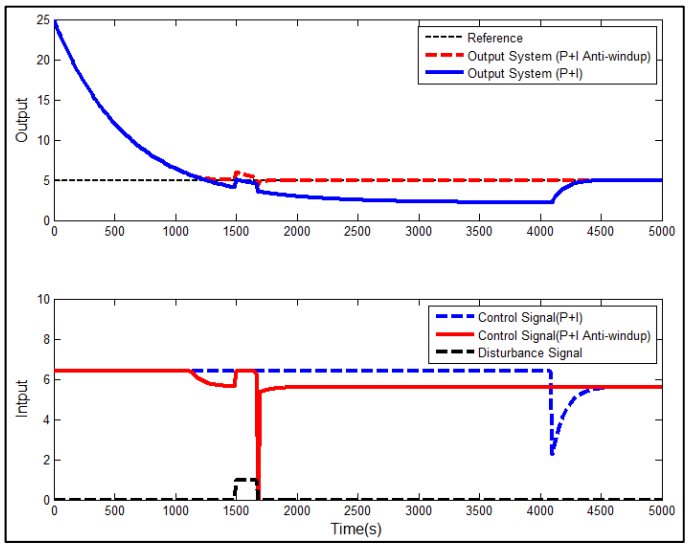


Figure 11. Disturbance Applicantion in the P+I Controller and in the Anti-windup P+I Controller with the Current Saturation.

## V. CONCLUSION

In this paper, it was mentioned that the temperature negatively influences the battery lifetime. The solution presented was the digital temperature control, which is easy to implement, has simple drive and low-cost with the use of Peltier thermoelectric modules.

For the control project, from experimental results, the system identification has been made, yielding a suitable model. The model was validated by means of a method for calculating the average error, obtaining a negligible value of only 0.89%.

It was compared the utilization of a conventional PI controller with the use of a P+I controller. It was observed that, as a slow system, the utilization of a controller which has a high control effort at the beginning of the reference implementation is more suitable, a characteristic that is observed in the P+I controller. Consequently, the rejection of the disturbance is faster, with a difference of about 4 minutes compared with the PI controller, as shown in Section IV.

With the insertion of the current saturation, the system output could present windup problem. To correct this problem, a structure was proposed with the P+I controller, according to

Figure 6. It was found that this change corrects the windup problem.

## REFERENCES


[1] C. Restrepo, A. Salazar, H. Schweizer and A. Ginart, "Residential Battery Storage: Is the Timing Right?," in *IEEE Electrification Magazine*, vol. 3, no. 3, pp. 14-21, Sept. 2015.

[2] "Global Solar Off-Grid Semi-Annual Market Report," GOGLA., May, 2016.

[3] P. Mints. (2013, August 21). Off-grid Solar Applications, Where Grid Parity Is Truly Meaningless [Online]. Available: http://www.renewableenergyworld.com/articles/2013/08/off-grid-solar-applications-where-grid-parity-is-truly-meaningless.

[4] N. Turman-Bryant, P. Alstone, D. Gershenson, D. M. Kammen, A. Jacobson, "The Rise of Solar: Market evolution of Off-Grid Lighing Three Kenyan Towns," Lighting Global, Oct, 2015.

[5] Handbook of Batteries, 3rd ed., McGraw-Hill., 2001, pp. 44–60.

[6] J. Leuchter and P. Bauer, "Capacity of power-batteries versus temperature," *Power Electronics and Applications (EPE'15 ECCE-Europe), 2015 17th European Conference on*, Geneva, 2015, pp. 1-8.

[7] Dongliang Zhao, Gang Tan, "A review of thermoelectric cooling: Materials, modeling and applications", *Applied Thermal Engineering*, Volume 66, Issues 1–2, May 2014, Pages 15-242

[8] S. McCluer, "Battery Technology for Data Centers and Network Rooms: Lead Acid Battery Options," APC, White Paper #30.

[9] C. M. T. Cruz *et al*., "Comparison of VRLA-AGM batteries lifetime charging with different currents waveforms for use on low power UPS," *2015 IEEE 13th Brazilian Power Electronics Conference and 1st Southern Power Electronics Conference (COBEP/SPEC)*, Fortaleza, 2015, pp. 1-6.

[10] S. Wen, G. Zhang, Y. Dan, D. Wang and M. Deng, "Model output following control for an aluminum plate cooling process with a Peltier device,"*The 2012 International Conference on Advanced Mechatronic Systems*, Tokyo, 2012, pp. 452-457.

[11] S. Lineykin and S. Ben-Yaakov, "Modeling and analysis of thermoelectric modules," *Twentieth Annual IEEE Applied Power Electronics Conference and Exposition, 2005. APEC 2005.*, 2005, pp. 2019-2023 Vol. 3.

[12] A. Ginart, A. Salazar, C. Restrepo, M. Geiger and H. Schweizer, "Thermoelectrical Management System for Stationary Outdoor Lithium-Ion Energy Storage," *2016 IEEE Green Technologies Conference (GreenTech)*, Kansas City, MO, 2016, pp. 78-83.

[13] C. Alaoui, "Solid-State Thermal Management for Lithium-Ion EV Batteries," in *IEEE Transactions on Vehicular Technology*, vol. 62, no. 1, pp. 98-107, Jan. 2013.

[14] S. Kumar, A. Gupta, G. Yadav and H. P. Singh, "Peltier module for refrigeration and heating using embedded system," *Recent Developments in Control, Automation and Power Engineering (RDCAPE), 2015 International Conference on*, Noida, 2015, pp. 314-319.

[15] C. Alaoui and Z. M. Salameh, "Solid state heater cooler: design and evaluation," *Power Engineering, 2001. LESCOPE '01. 2001 Large Engineering Systems Conference on*, Halifax, NS, 2001, pp. 139-145.

[16] A. A. R. Coelho and L. S. Coelho, "Identificação de Sistemas Dinâmicos Lineares", in *UFSC. Florianópolis, 2004.* pp 9-11; 49.

[17] I. D. Landau and G. Zito, "Digital Control Systems: Design, Identificaton and Implentation", in *Springer. London, 2006.* pp 1-7; 87-92; 202.

[18] Hebei I. T. Co., Ltd. (2015, August 10). *TEC1 – 12706 (2.03 ed.)* [Online]. Available: http://www.hebeiltd.com.cn.

[19] Texas Instruments. (2016, January 3). *LM35 Precision Centigrade Temperature Sensors (2nd ed.).* [Online]. Available: http://www.ti.com.

[20] K. Ogata, "Análise de Resposta Transitória e de Regime Estacionário", in Engenharia de Controle Moderno, 5th ed. São Paulo, Brazil: Pearson, 2007, pp. 158.

[21] D. S. Silva, F. V. Alvarado and M. C. M. Teixeira, "Identificação de Funções de Transferência Utilizando como Entrada um Degrau", Ilha Solteira, Brasil, 2012, Ch 2, pp. 29-32.